AIMS Materials Science, 6(2): 276–287.
DOI: 10.3934/matersci.2019.2.276
Received: 28 December 2018
Accepted: 24 March 2019
Published: 03 April 2019

http://www.aimspress.com/journal/Materials

Research article

The properties study of transparent conductive oxides (TCO) of tin dioxide (ATO) doped by antimony obtained by spray pyrolysis

Timur Zinchenko, Ekaterina Pecherskaya* and Dmitriy Artamonov

Department of Information measuring equipment and metrology, Penza State University, 440026, Penza, Russia

*** Correspondence:** Email: pea1@list.ru; Tel: +78412368221; Fax: +78412552776.

Abstract: Transparent conductive coatings based on thin films of metal oxides are widely used in various optoelectronic devices and appliances. The article is devoted to the study of the morphological, structural, electrical and optical properties of transparent conductive oxide. Tin dioxide thin films are obtained by spray pyrolysis technique on glass substrates. Analysis of the structural properties showed that SnO_2 has a tetragonal crystal structure. Analysis of the morphological properties showed that the grain size of the films increases at a deposition temperature from 450 to 550 ℃. Dependencies of the transmittance coefficient of samples obtained on the solutions volume and transmittance coefficient of samples obtained on the doping levels have become the result of studying the optical properties of transparent conductive oxide. The transmittance is almost independent on the amount of substance sprayed onto the substrate. However, the transmittance is greatly influenced by the chemical composition of the films. The main electrical parameter affecting the TCO quality is conductivity or surface resistance. Surface resistance is measured by probe methods, the most accurate of which is the Van der Pauw method. Surface resistance consistently decreases with increasing solution volume, precursor concentration and impurity concentration.

Keywords: transparent conductive oxide; spray pyrolysis; tin dioxide; precursor; structural properties; conductivity; surface resistance; optical transparent

1. Introduction

Transparent conductive oxides are metal oxides with high electrical conductivity and

transparency in the visible and near infrared regions of the light wavelengths. By themselves, metal oxides, such as In_2O_3, SnO_2, ZnO, etc., are dielectrics. But due to the large number of defects, namely oxygen vacancies, they conduct electricity, which makes them, in fact, wide-gap semiconductors [1]. To achieve the necessary conductivity values, the introduction of a doping impurity is used, and the impurity valence must be higher than the valence of the metal atom that forms the oxide compound, which will make it possible to obtain n-type conductivity [2,3]. High transparency (>80%) in the visible region of the spectrum and the near infrared region is explained by the appearance of a plasma edge. Light is reflected due to the fact that the light frequency ω coincides with the frequency of collective oscillations of charge carriers in a material (plasma frequency ω_p):

$$\omega_p = \left(\frac{n \cdot e^2}{\varepsilon_0 \cdot \varepsilon_\infty \cdot m^*} \right)^{1/2} \quad (1)$$

where n is the concentration of charge carriers, e is the electronic charge, ε_0 is the permittivity of free space, ε_∞ is the high-frequency permittivity and m^* is the effective electron mass. While the light transmission in the near ultraviolet ($\lambda < 350$ nm) is restricted by the forbidden band, since photons with energy $\hbar\omega > E_g$ are absorbed.

Transparent conductive oxide (TCO) are widely used: solar cells, gas sensitive sensors, liquid crystal displays, touch-screens, smart glasses and other optoelectronic and semiconductor devices and tools [4–7]. However, the most widely used material today is indium tin oxide or ITO coating. The conductivity and transparency of this material are currently the highest, but the main drawback is its high cost due to the indium shortage on the planet. Many scientists are trying to find a replacement for this material and in this work an alternative material is considered, namely antimony tin oxide, since it has the following characteristics: it is sufficiently resistant to atmospheric conditions, chemically inert and can withstand high temperature, has a low cost, but the conductivity of these materials has not yet reached the level that ITO has [8]. At the same time, the method of spray pyrolysis or aerosols pyrolysis was used to further reduce the cost, facilitate the technological process and the possibility of applying large areas (for example, for smart glasses).

2. Materials and method

Since transparent conductive coatings are used most often coatings on glasses, soda-calcium-silicate glasses are chosen as substrates for the preparation. Sample size is 2.5 cm by 2.5 cm. The process of obtaining TCO samples based on tin dioxide in the spray pyrolysis technology framework consisted of several stages: surface preparation of glass substrates; preparation of precursor solutions; deposition of pure and antimony doped tin dioxide films on the surface of the substrates [9]. Before placing the substrates in the reaction chamber of the installation, their surface was cleaned from possible contaminants that adversely affect the adhesion strength (adhesion). The following substances were used to prepare the substrates: distilled water; baking soda—sodium bicarbonate ($NaHCO_3$); ethanol (C_2H_5OH); chromic mixture (mixture of concentrated sulfuric acid (H_2SO_4) and potassium dichromate ($K_2Cr_2O_7$)). The most important operations in preparing the substrate are ultrasonic substrates processing in ethanol and substrates processing in a heated chromium mixture. The second step is the precursors solutions preparation. The following

substances were used: precursor № 1—tin tetrachloride ($SnCl_4$ $5H_2O$); precursor № 2—antimony trichloride ($SbCl_3$); the solvent is ethanol (C_2H_5OH).

The choice of precursors is due to the following: to obtain tin oxide, tetrachloride tin pentahydrate was chosen since the formation of an oxide film occurs due to the surface hydrolysis of metal chloride on the heated surface of the substrate. Getting it by this way is most suitable for the use of the method of aerosols pyrolysis. The method of hydrolysis of solutions of chlorine tin is convenient for approbation and selection of the amount and type of alloying additives to SnO_2 It is also worth noting that alcohol solutions should be used as a solvent; aqueous solutions can cause cracking of substrates [10].

The formation of a metal oxide film from, for example, chloride can be described by the following equation:

$$XCl_m + nH_2O = XO_n + mHCl \tag{2}$$

where X is a metal (Sn, Zn, Cu, etc.).

As for antimony trichloride, the precursor is chosen as it allows to obtain antimony with a purity of 99.999%. At the same time, antimony in its pure form is a toxic material, this problem is described in [11,12].

Antimony itself is chosen as an impurity due to the fact that the results of conductivity and transparency of tin oxide coatings with antimony have high enough indicators for the use as transparent conductive oxides [13].

To obtain a solution, it is necessary to calculate the precursors mass. The mass of precursor № 1 m_{prec1} for the preparation of a solution with a volume of V_{rast} = 60 mL with a molar concentration of C_M = 0.25 mol/L was calculated by the formula:

$$m_{prec1} = C_M \cdot V_{rast} \cdot M_{prec1} \tag{3}$$

where M_{prec1} is the molar mass of precursor № 1.

To ensure different levels of tin dioxide films doping, the mass of precursor № 2 was used for different values of the mole fraction of antimony trichloride N_{prec2} = (0.001; 0.0005; 0.00025) in the resulting solution. Mass was according by the following formula:

$$m_{prec2} = n_{prec2} \cdot M_{prec2} \tag{4}$$

where n_{prec2} is the quantity of precursor № 2 substance; M_{prec2} is molar mass of precursor № 2.

Since the mole fraction of a solution component is equal to the ratio of the substance amount of a given component to the total substance amount of all components in a solution, the values of n_{prec2} were calculated according to the following expression:

$$n_{prec2} = \frac{N_{prec2}\left(n_{C2H5OH} + n_{prec1}\right)}{1 - N_{prec2}} \tag{5}$$

The calculated mass values at the corresponding precursor № 2 concentrations are presented in Table 1.

Table 1. Mass and concentration of antimony trichloride precursor.

m_{prec2}, g	N_{prec2}, %
0.055	0.025
0.11	0.05
0.22	0.1

The deposition of tin dioxide films with different levels of antimony doping was carried out sequentially in a spray pyrolysis installation. Table 2 shows the values of the technological parameters for which TCO samples are obtained on the basis of tin dioxide. It should be noted that the optimal values of the parameters Ts (heater temperature), C_M (concentration of precursor № 1), l (distance between the sprayer and the substrate), p (inlet air pressure in the sprayer) were chosen as a result of numerous experiments aimed at achieving the minimum surface resistance R_S of SnO_2 coated samples.

Table 2. Technological modes of application.

Parameter	Value
substrate material	soda-lime-silica glass
precursor № 1	$SnCl_4$ $5H_2O$
precursor № 2	$SbCl_3$
solvent	ethanol
carrier gas	compressed air
C_M (concentration of precursor № 1)	0.25 mol/L
N_{prec2} (concentration of precursor № 2)	0.1, 0.05, 0.025 mol%
V_{rast} (volume of solutions)	5–20 mL
l (distance between the sprayer and the substrate)	300 mm
p (inlet air pressure in the sprayer)	2 bar
Ts (heater temperature)	300–550 ℃

3. Results

3.1. Structure

Figure 1 shows the phase composition of the obtained tin dioxide films doped by antimony.

Analysis of the diffraction pattern of the phase film composition showed that the thin-film structure is polycrystalline. Comparison and analysis of the obtained results confirm that SnO_2 has a tetragonal crystal structure. The structure of the coating is significantly affected by the pyrolysis temperature. As a result of the experiment, ATO samples were obtained at different values of the pyrolysis temperature. Studies have shown that the optimal temperature of pyrolysis is a temperature equal to 450 ℃ [14].

Pyrolysis temperature plays a key role in the mechanism for producing a thin film. Analysis of the diffractogram showed that the following crystallographic directions were present: 200, 211, 110, 101. Moreover, strong intense reflection is observed along 200 and 211. In this case, less strong

peaks are observed at directions 110 and 101. The obtained diffraction pattern interpretation corresponds to the standard random orientation of polycrystalline SnO_2 [15].

With an increase in the deposition temperature from 450 to 550 ℃, there is an increase of the film thickness and grain size. The orientation also changes from the crystallographic direction 200 to the crystallographic direction 211. It is also worth to note that the grain size of the films increases at a deposition temperature from 450 to 550 ℃ [16].

Sb impurity concentrations in tin dioxide are ranged: for the first sample from 0.015 to 0.025%, for the second sample from 0.043 to 0.051%, for the third sample from 0.088 to 0.1%. The measurement method is similar to that used in [17]. The results are given taking into account the measurement errors.

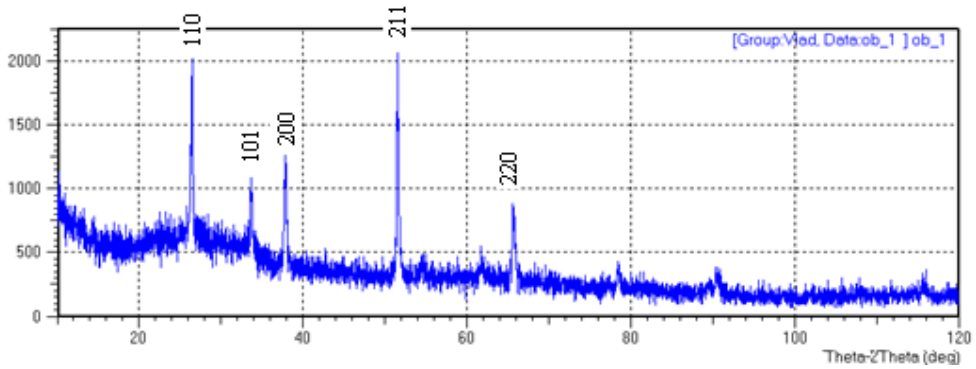

Figure 1. Diffraction pattern of samples with ATO coating at a pyrolysis temperature of 450 ℃.

3.2. Morphology

Figure 2 shows the SEM images of ATO coatings obtained at different pyrolysis temperatures and having different thicknesses.

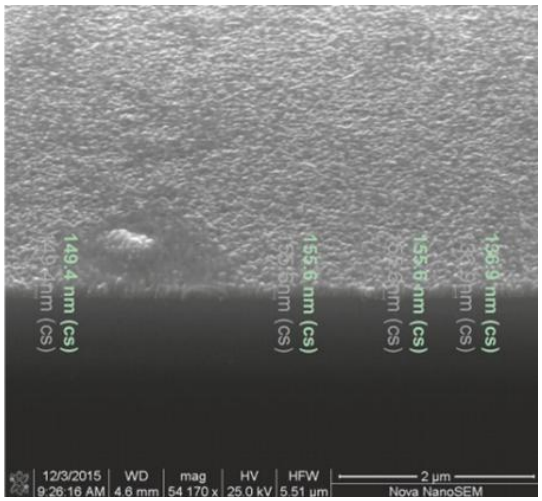

(a) pyrolysis temperature 400 °C

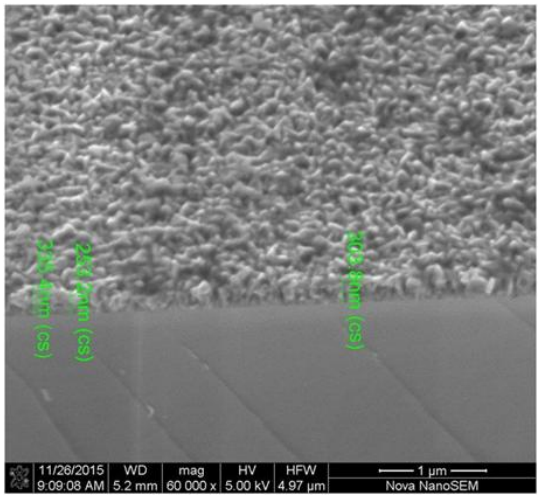

(b) pyrolysis temperature 450 °C

Figure 2. SEM image of ATO coatings.

The images can be concluded that the films are homogeneous and have good adhesion. It is worth to note that at a temperature of 450 ℃, pyramidal crystals predominate (Figure 3). When the temperature rises, needle and prismatic crystals appear. The most high-quality structure of the coating should have a dieteragonally-dipyramidal form of the system. This means that macrocrystals represent structures from a combination of a prism and a pyramid.

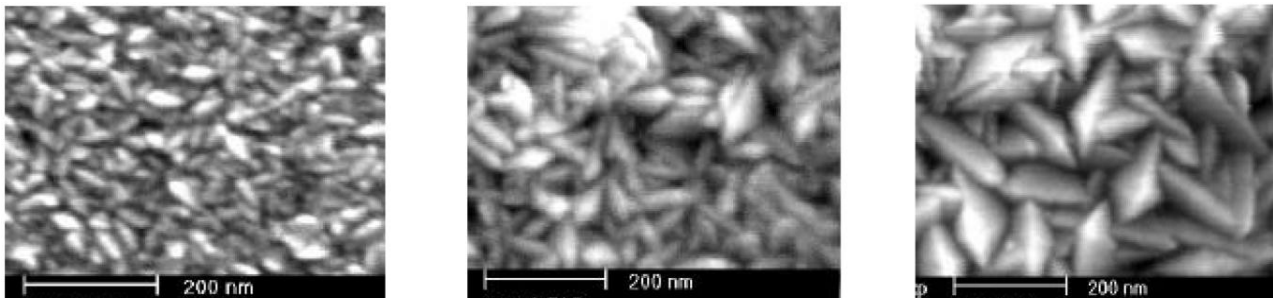

(a) d = 37 nm (b) d = 170 nm (c) d = 300 nm

Figure 3. SEM image of ATO coatings at different thicknesses and pyrolysis temperatures 450 ℃.

The coating thickness also affects the coating structure, namely the crystals size. The change nature of the film structure with a change in thickness can be considered as evidence that film growth occurs layer by layer during deposition. This means that when a certain thickness is reached, the crystallites cease to grow, and then new crystallites are formed on their surface. In other words, films can have a layered structure, where each layer has its own structure with a different crystallite size and their preferred orientation. Dependences presented in Figure 4 confirm this. A structure analysis of tin dioxide films also shows that amorphous films are formed at Ts < 300 ℃ and polycrystalline films at Ts > 350 ℃ [18–20].

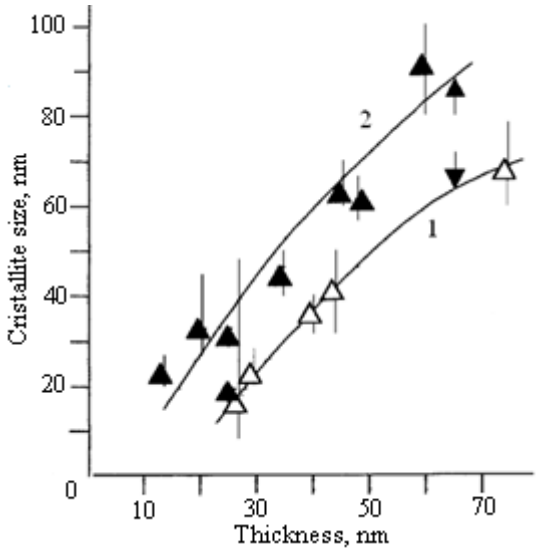

Figure 4. Dependence of crystallite size on SnO_2 film thickness. 1: Ts = 450 ℃; 2: Ts = 530 ℃.

3.3. Optical properties

Transparent conductive oxides should be transparent in the visible region of the spectrum, usually defined in the range of 400–750 nm [21]. Light with the energy above the band gap is absorbed during transitions. This is due to a sharp decrease in transmittance and increased absorption at shorter wavelengths (less than 350 nm). Conventional transparent conductive materials have a band gap greater than 3 eV. Figure 5 shows the dependence of the transmittance coefficient of the films on the wavelength for pure tin dioxide with a different volume of the sprayed solution. The samples characteristics are presented in Table 2.

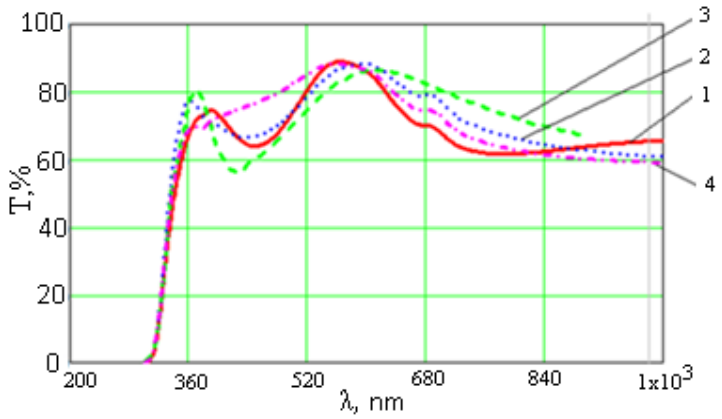

Figure 5. Transmittance coefficient of samples obtained with different volume of solutions. 1: volume of solution 20 mL; 2: volume of solution 15 mL; 3: volume of solution 10 mL; 4: volume of solution 5 mL.

According to Figure 5, the transmittance is almost independent on the amount of substance sprayed onto the substrate. However, the transmittance is greatly influenced by the chemical films composition. Figure 6 shows the dependence of the transmittance at various impurity concentrations.

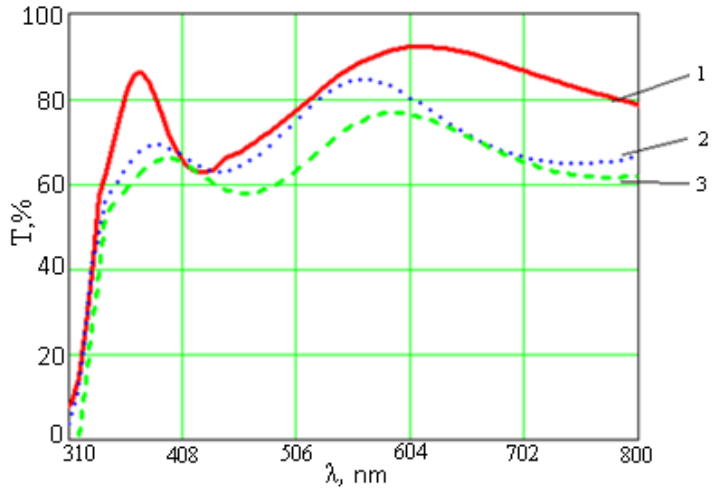

Figure 6. Transmittance coefficient of samples obtained with different doping levels (volume 10 mL). 1: 0% doping; 2: 0.1% doping; 3: 0.25% doping.

When an impurity is introduced into the semiconductor, the charge carrier concentration in the TCO will lead to a change in the plasma frequency. As the charge carrier concentration in the TCO increases, the plasma frequency will shift towards the visible range, and the corresponding transparency window will decrease significantly. Plasma frequency and concentration of charge carriers in the material is related as follows [22]:

$$\omega_{\rho=}\left(\frac{ne^2}{m^*\varepsilon_0\varepsilon_\infty}\right)^{1/2} \quad (6)$$

where n is the concentration of free charge carriers, e is the electron electric charge (1.6×10^{-19} C); m* is the effective electron mass in a material, ε_0 is the electric constant (8.85×10^{-12} F/m), ε_∞ is the dielectric constant of the material at high frequencies.

Electromagnetic waves of lower frequency are absorbed by the material, and for waves of higher frequency it becomes much more transparent. In practice, it is more convenient to use the plasma length, which is easier to calculate as [23,24]:

$$\lambda = \sqrt{\frac{4\pi \cdot c^2}{\omega_p^2}} \quad (7)$$

The results of the plasma frequency and the plasma wavelength are presented in Table 3.

3.4. Electrical properties

The main electrical parameter affecting the TCO quality is conductivity or surface resistance. Surface resistance is measured by probe methods, the most accurate of which is the Van der Pauw method [25]. The results are in Table 3.

Table 3. The surface resistance of the samples obtained by the Van der Pau method.

Sample, №	Thickness, nm	Surface Resistance, Ω/□	Plasma frequency, Hz	Plasma wavelength, μm
1	115	1463	9.13×10^{14}	2.07
2	133	841	3.224×10^{14}	5.8
3	168	667	2.5×10^{14}	7.5
4	209	624	3.09×10^{14}	6.1

Surface resistance is used to indirectly measure electrical parameters such as resistivity and mobility of charge carriers in ATO films at room temperature. Indicators of carrier concentration and mobility range from 5.31×10^{19} to 7.08×10^{20} cm^{-3} and from 8.03 to 13.25 cm^2/V s, respectively. A gradual increase of mobility may be associated with a decrease of the boundary potential due to the improved films crystallinity. For a complete picture, it is necessary to calculate the Fermi energy, as well as the mean free path.

The Fermi energy is the maximum energy of electrons at an absolute zero temperature. The Fermi energy is calculated by the formula [26]:

$$E_f = (\frac{h^2}{m^*})(\frac{3n}{\pi})^{2/3} \quad (8)$$

where h is the constant bar, m* is the effective electron mass, n is the concentration of charge carriers. The results of determining the parameters of 4 samples of coatings are represented in Table 4. The obtained results of resistivity measurements are of the same order as for the samples of polycrystalline SnO_2 thin films [27]. At the same time, the resistivity of the F-doped SnO_2 samples according to the article [28] at room temperature is almost an order of magnitude lower than that of the samples of tin dioxide doped by antimony. The mean free path is the distance that an electron overcomes without scattering (from scattering to scattering). This indicator is calculated using the following expression [16]:

$$L = \mu \frac{h}{2e} \left(\frac{3n}{\pi}\right)^{1/3} \tag{9}$$

Table 4. Electrophysical parameters of the obtained samples of synthesized transparent conductive coatings.

Sample, №	Resistivity, Ω cm	Specific conductivity, $\frac{1}{\Omega \cdot cm}$	Carrier mobility, $cm^2/V\ s$	Volume concentration, cm^{-3}	Surface concentration, cm^{-2}	Free path length, m	Fermi energy, J
1	6.67×10^{-3}	150	13.25	7.08×10^{20}	7.08×10^{14}	2.406×10^{-9}	3.451×10^{-19}
2	6.24×10^{-3}	160	11.34	8.83×10^{19}	8.83×10^{15}	1.029×10^{-9}	8.615×10^{-20}
3	1.46×10^{-2}	68.4	8.03	5.31×10^{19}	5.31×10^{14}	6.149×10^{-10}	6.137×10^{-20}
4	8.41×10^{-3}	119	9.15	8.11×10^{19}	8.11×10^{14}	8.069×10^{-10}	8.14×10^{-20}

Figures 7 and 8 show the dependence electrical properties for the conditions of obtaining.

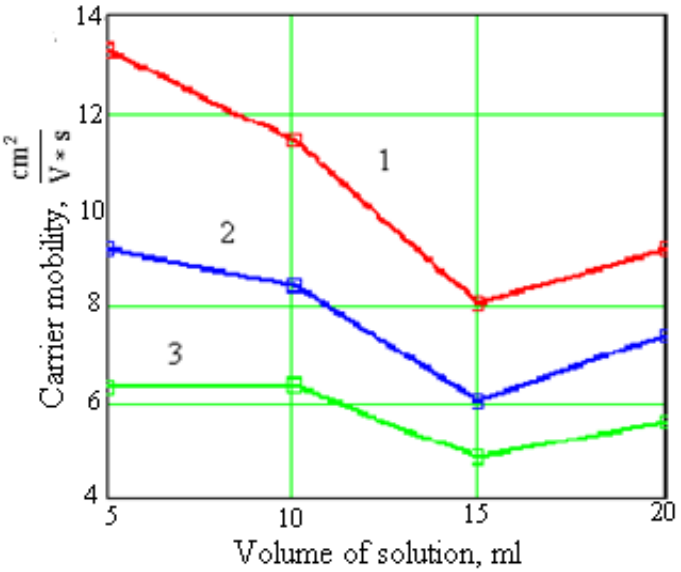

Figure 7. Dependence of carrier mobility on the solution volume. 1: impurity concentration 0%; 2: impurity concentration 5%; 3: impurity concentration of 10%.

The mobility of the carriers decreases with an increase in the volume of the solution to a certain

value, and then increases. This is due to carrier scattering, which, up to a certain value of the solution volume, is noticeably manifested, then decreases. All readings were obtained with readings of the concentration of precursor № 1 C_M = 0.25 mol/L.

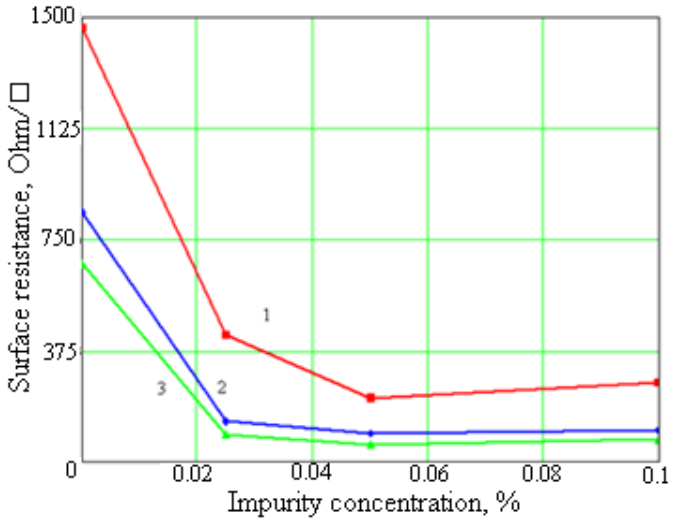

Figure 8. Dependence of surface resistance on impurity concentration. 1: volume of solution 5 mol/L; 2: volume of solution 10 mol/L; 3: solution volume 15 mol/L.

The surface resistance decreases with increasing solution volume, precursor concentration and impurity concentration. Surface resistance decreases with increasing impurity concentration (antimony). Antimony replaces tin atoms in the lattice [29]. As a result, antimony atoms act as donors and create an excess amount of free electrons. A slight increase in the value of R_S above a certain doping concentration is due to the fact that excess antimony atoms do not occupy the correct positions in the lattice, which leads to disruption of the structure and an increase in surface resistance.

4. Conclusion

The pyrolysis temperature has a significant effect on the coating structure. The optimum temperature is 450 ℃. The coating thickness also affects the coating structure, namely the crystals size. The transmittance is almost independent on the amount of substance sprayed onto the substrate. However, the transmittance is greatly influenced by the chemical composition of the films. Surface resistance consistently decreases with increasing solution volume, precursor concentration and impurity concentration.

Conflict of interest

The authors declare no conflict of interest.

References

1. Raksha SV, Kondrashin VI, Pecherskaya EA, et al. (2015) Functional materials for dye-sensitized solar cells. *J Nano- Electron Phys* 7: 04062.
2. Kawazoe H, Yanagi H, Ueda K, et al. (2000) Transparent *p*-type conducting oxides: design and fabrication of *p-n* heterojunctions. *MRS Bull* 25: 28–36.
3. Gordon RG (2000) Criteria for choosing transparent conductors. *MRS Bull* 25: 52–57.
4. Lewis BG, Paine DC (2000) Applications and processing of transparent conducting oxides. *MRS Bull* 25: 22–27.
5. Porch A, Morgan DV, Perks RM, et al. (2004) Electromagnetic absorption in transparent conducting films. *J Appl Phys* 95: 4734–4737.
6. Tiwari AN, Khrypunov G, Kurdzesau F, et al. (2004) CdTe solar cell in a novel configuration. *Prog Photovoltaics* 12: 33–38.
7. Hamberg I, Granqvist CG (1986) Evaporated Sn-doped In_2O_3 films: basic optical properties and applications to energy-efficient windows. *J Appl Phys* 60: R123–R160.
8. Batzill M, Diebold U (2005) The surface and materials science of tin oxide. *Prog Surf Sci* 79: 47–154.
9. Zinchenko TO, Kondrashin VI, Pecherskaya EA, et al. (2017) Electrical properties of transparent conductive ATO coatings obtained by spray pyrolysis. *IOP Conference Series: Materials Science and Engineering*, 225: 012255.
10. Rembeza SI, Svistova TV, Rembeza ES, et al. (2004) Electric and optical properties of semiconductor films based on SnO_2 and SiO_2. *Russ Electr Eng* 75: 11–15.
11. Biswas P, Wu CY (1998) Control of toxic metal emissions from combustors using sorbents: a review. *J Air Waste Manage* 48: 113–127.
12. Linak WP, Wendt JOL (1993) Toxic metal emissions from incineration: Mechanisms and control. *Prog Energ Combust* 19: 145–185.
13. Elangovan E, Ramamurthi K (2005) A study on low cost-hight conducting fluorine and antimony-doped tin oxide thin films. *Appl Surf Sci* 249: 183–196.
14. Patil GE, Kajale DD, Chavan DN, et al. (2011) Synthesis, characterization and gas sensing performance of SnO_2 thin films prepared by spray pyrolysis. *B Mater Sci* 34: 1–9.
15. Vincent CA, Weston DGC (1972) Preparation and properties of semiconducting polycrystalline tin oxide. *J Electrochem Soc* 119: 518–521.
16. Babar AR, Shinde SS, Moholkar AV, et al. (2011) Structural and optoelectronic properties of sprayed Sb:SnO_2 thin films: Effects of substrate temperature and nozzle-to-substrate distance. *J Semicond* 32: 102001.
17. Dominguez JE, Sun HP, Pan XQ (2002) Aliovalent dopant distribution in nanocrystalline tin dioxide thin films studied by X-ray energy dispersive spectroscopy. *Microsc Microanal* 8: 1168–1169.
18. Korotcenkov G, Brinzari V, Schwank J, et al. (2001) Peculiarities of SnO_2 thin film deposition by spray pyrolysis for gas sensor application. *Sensor Actuat B-Chem* 77: 244–252.
19. Katerynchuk VM, Kovalyuk MZ (2010) Films of degenerate intrinsic oxides of InSe and In_4Se_3 semiconductor crystals. *Semiconductors* 44: 1176–1179.
20. Sidelev DV, Yurjev YN (2014) The reactive deposition of TiO_x thin films. *Adv Mater Res* 1040: 748–752.

21. Ginley DS, Hosono H, Paine DC (2010) *Handbook of transparent conductor*s, Springer.
22. Solieman A, Aegerter MA (2006) Modeling of optical and electrical properties of In_2O_3:Sn coatings made by various techniques. *Thin Solid Films* 502: 205–211.
23. Meng LJ, Dos Santos MP (1997) Properties of indium tin oxides (ITO) films prepared by r.f. reactive magnetron sputtering at different pressures. *Thin Solid Films* 303: 151–155.
24. Meng LJ, Gao J, Dos Santos MP, et al. (2008) The effect of the ion beam energy on the properties of indium tin oxide films prepared by ion beam assisted deposition. *Thin Solid Films* 516: 1365–1369.
25. Zinchenko TO, Pecherskaya YA, Kondrashin VI, et al. (2017) Analysis of research methods of electro-physical properties of transparent conducting coatings received by spray pyrolysis. *18th International Conference of Young Specialists on Micro/Nanotechnologies and Electron Devices (EDM)*, 320–323.
26. Conwell E, Weisskopf VF (1950) Theory of impurity scattering in semiconductors. *Phys Rev* 77: 388.
27. Li QL, Zhang XH, Lin T, et al. (2018) Electrical transport properties of polycrystalline SnO_2 thin films. *J Alloy Compd* 764: 295–299.
28. Gao KH, Lin T, Liu XD, et al. (2013) Low temperature electrical transport properties of F-doped SnO_2 films. *Solid State Commun* 157: 49–53.
29. Dudnik EV, Lakiza SN, Tishchenko YS, et al. (2014) Phase diagrams of refractory oxide systems and microstructural design of materials. *Powder Metall Met C* 53: 303–311.

AIMS Press